International Journal of Fatigue 95 (2017) 8–17

Contents lists available at ScienceDirect

International Journal of Fatigue

journal homepage: www.elsevier.com/locate/ijfatigue

A combined critical distance and highly-stressed-volume model to evaluate the statistical size effect of the stress concentrator on low cycle fatigue of TA19 plate

Rongqiao Wang [a,b,c], Da Li [a], Dianyin Hu [a,b,c,*], Fanchao Meng [d], Hui Liu [a], Qihang Ma [a]

[a] School of Energy and Power Engineering, Beihang University, Beijing 100191, China
[b] Collaborative Innovation Center of Advanced Aero-Engine, Beijing 100191, China
[c] Beijing Key Laboratory of Aero-Engine Structure and Strength, Beijing 100191, China
[d] Mining and Materials Engineering, McGill University, Montreal, QC H3A 0C5, Canada

ARTICLE INFO

Article history:
Received 3 July 2016
Received in revised form 2 October 2016
Accepted 3 October 2016
Available online 5 October 2016

Keywords:
Statistical size effect
Critical distance
Low cycle fatigue
Life prediction
Stress concentration
Highly-stressed-volume

ABSTRACT

Titanium alloy has been widely used for compressor discs in aero-engines due to its high specific strength. As a common geometry feature in compressor discs, bolt hole with stress concentration can cause compressor discs to fail under low cycle fatigue (LCF). In this study, the statistical size effect of such stress concentrators was investigated by LCF experimentations and theoretical predictions for titanium alloy plate specimens with a central circular hole (CHP). Four different scales of test sections without the influence of geometrical size were specially designed and experimental tests were conducted under LCF loading at 180 °C. The strain-controlled LCF tests of smooth specimen were also carried out at the same temperature. It is found that the predicted LCF lifetime from the theory of critical distance (TCD) correlates well with experimental results for the 100%-scale CHP specimens. However, it fails to accurately predict the dependence of LCF lifetime on the statistical size effect for CHP specimens at the other scales i.e., 40%-scale, 60%-scale, and 80%-scale. Furthermore, a novel methodology combining the TCD and highly-stressed-volume models is proposed to evaluate the statistical size effect, which exhibits much improved accuracy than the TCD method alone. The new model not only inherits the versatility of the TCD method but providing an essential assessment of the statistical size effect.

1. Introduction

Compressor disc often made of titanium alloy is a critical component of an aero-engine. During service, it undergoes significant centrifugal loading and generally fails under low cycle fatigue (LCF), which usually occurs in the typical geometry feature of compressor disc, such as bolt holes that are acting as local stress concentrators [1,2]. In addition, the local stress concentrators for the compressor discs may feature different geometrical shapes and sizes in order to satisfy the design requirements. Kloos [3] classified the origins of stress concentrators into several aspects, i.e., (i) geometrical size effect attributed to stress inhomogeneity from different notch types, (ii) statistical size effect induced by the high probability of defects in larger specimens, (iii) production size effect generated by the production technology (like residual stress), and (iv) surface size effect caused by the surface technology (such as the roughness). Therefore, it has triggered enormous research efforts to incorporate the stress concentration phenomenon (i.e., notch effect) in evaluating fatigue lifetime to ensure reliable life prediction for the aerospace industry [4].

It is demonstrated that traditional fatigue life prediction method based on the maximum stress or strain at the hole, is often inadequate to evaluate the fatigue life of the components with stress concentration features. As such, several methods have been discovered to investigate the effect of notches on the fatigue life. Among the commonly used strategies [5–8], the theory of critical distance (TCD), which evaluates the fatigue property based on effective stress/strain around the stress concentrator [9], is employed in the present work because of its versatility. For example, it has been reported that TCD method can successfully predict fatigue life of notched specimens subjected to variable amplitude fatigue loading [10,11], torsional loading [12], and dynamic loading [13]. Despite that there are many studies reported by using the TCD method to examine the size effect of different notch types on fatigue life prediction [14–17], the statistical size effect on the

* Corresponding author at: School of Energy and Power Engineering, Beihang University, Beijing 100191, China.
E-mail address: hdy@buaa.edu.cn (D. Hu).

http://dx.doi.org/10.1016/j.ijfatigue.2016.10.003
0142-1123/

Nomenclature

Symbols

A	material constant in TCD
B	material constant in TCD
b	fatigue strength exponent
C	material constant in LNV model
c	fatigue ductility exponent
E	Young's modulus
$\overline{E}$	average absolute error
E_i	absolute error
K_t	stress concentration factor
L	critical distance
N_f	fatigue life
$N_{f,1}$	initial value of fatigue life
$N_{f,2}$	calculated value of fatigue life
N_p	predicted fatigue life
$N_{p,i}$	predicted fatigue life for the ith data
N_e	experimental fatigue life
$N_{e,i}$	experimental fatigue life for the ith data

Abbreviations

PM	point method
FE	finite element
CHP	plate with a central circular hole
TCD	theory of critical distance
SWT	Smith-Watson-Topper
LCF	low cycle fatigue
LNV	combined critical distance and highly-stressed-volume model
ΔN	life scatter factor
R_σ	stress ratio
R_ε	strain ratio
V_0	reference volume
V_{90}	volume with $\sigma_a \geqslant 0.9\sigma_{a,max}$
ε'_f	fatigue ductility coefficient
$\Delta\varepsilon_t$	total normal strain range
$\sigma_{0.2}$	0.2% offset yield stress
σ_A	fatigue strength
σ_{A0}	reference fatigue strength
σ_a	stress amplitude
$\sigma_{a,max}$	maximum stress amplitude
σ_b	ultimate tensile strength
σ_m	mean stress
σ_{max}	maximum tensile stress
σ'_f	fatigue strength coefficient
v	material coefficient in V90 criterion

notch fatigue cannot be overlooked since the larger the specimen is, the more initiated cracks will be found, and thereby the higher probability and the shorter fatigue life appears even under the same fatigue loading. To this end, Makkonen [18,19] experimentally demonstrated the significant influence of statistical size on the high cycle fatigue (HCF) lifetime for both the smooth and grooved cylindrical specimens. Moreover, due to its significance to structural reliability, many design standards require the consideration of statistical size effect [20–22]. However, currently it largely remains elusive that how the statistical size of the stress concentrators will affect the LCF lifetime of compressor disc made of titanium alloy. Therefore, in this study we performed in-depth work to assess the statistical size effect on the LCF lifetime of an actual compressor disc made of TA19 titanium alloy, and aim to develop a predictive model to evaluate such effect based on systematic experimentations of notch fatigue under LCF loading.

This paper is outlined as follows: strain-controlled LCF tests were firstly conducted on smooth specimens to establish the LCF life model of the TA19 material based on Smith-Watson-Topper (SWT) parameter. Then, the LCF experiments were conducted on a broad range of geometry scales of plates with a central circular hole (CHP specimens) to investigate the statistical size effect of the bolt hole on the LCF lifetime. Finally, a combination of the critical distance with highly-stressed-volume model was proposed to describe the dependence of the LCF lifetime on the statistical size effect.

2. Experimental details

2.1. Material

The chemical composition of TA19 titanium alloy is (in wt%): 6.0Al; 2.0Sn; 4.0Zr; 2.0Mo; 0.08Si; balance Ti. The mechanical properties, including the Young's modulus E, the 0.2% offset yield stress $\sigma_{0.2}$, and the ultimate tensile strength σ_b, under different testing temperatures are listed in Table 1.

Table 1
Mechanical properties for TA19 alloy.

Temperature (°C)	E (GPa)	$\sigma_{0.2}$ (MPa)	σ_b (MPa)
20	119.2	1015	1100
100	113.3	920	1025
180	109.8	825	953
300	104.0	720	875

2.2. Specimen geometry

All specimens under the LCF experiments were cut from an actual compressor disc. The compressor disc was solution heat treated at a temperature of 980 °C and held for 100 min, followed by an air cool. Afterwards, the compressor disc underwent an aging heat treatment at 720 °C for 520 min, after which it was cooled to 620 °C at a rate of 50 °C/h and then held for 480 min, followed by an air cool.

The geometry of the smooth specimen is shown in Fig. 1. In order to investigate the statistical size effect on the LCF lifetime, different scales of CHP specimens were designed, as shown in Fig. 2. The 100%-scale CHP specimen (see Fig. 2(a)) has the same notch dimension (i.e., the thickness, hole diameter, and chamfer)

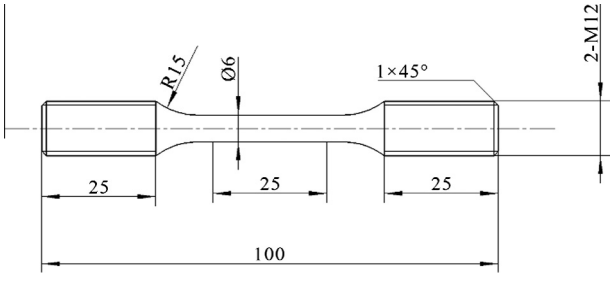

Fig. 1. Smooth specimen (unit: mm).

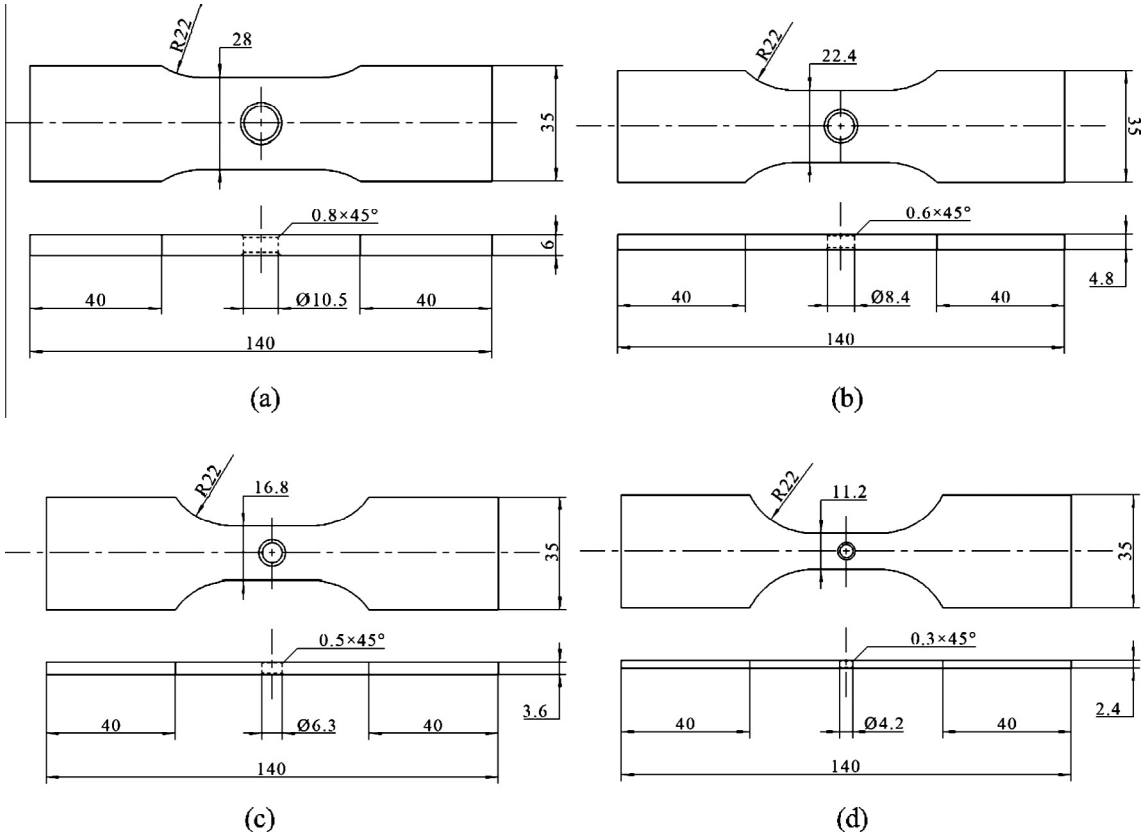

Fig. 2. CHP specimens with different scales of test sections (unit: mm): (a) 100%-scale specimen, (b) 80%-scale specimen, (c) 60%-scale specimen, and (d) 40%-scale specimen.

as the bolt hole in the compressor disc. Then the gauge width was determined using linear-elastic finite element (FE) analysis to ensure similar stress field to the bolt hole in the compressor disc at service. In addition, other CHP specimens with three different scales of test sections were designed, i.e., 80%-scale specimen, 60%-scale specimen and 40%-scale specimen, which means that the thickness, hole diameter and width of the test section were reduced to 80%, 60% and 40% of the 100%-scale CHP specimen, as shown in Fig. 2(b)–(d). Accordingly, the chamfers around the hole were 0.6 mm, 0.5 mm, and 0.3 mm, respectively. The above design ensures the stress concentration factor of all CHP specimens in different scales to be nearly equal to effectively exclude the geometrical size effect when comparing with experimental results (see Supplementary material for details).

2.3. Procedures of LCF test

The LCF tests were conducted on a 100 kN servo-hydraulic testing machine with a triangular waveform. The LCF tests on the CHP specimens were conducted at a stress ratio $R_\sigma = 0.1$ and a frequency $f = 3$ Hz. The loading levels of CHP specimens were relatively high with necessarily plastic strain on the hole tip. According to the previous work by Manson and Coffin [23,24], strain is the dominant damage parameter in LCF regime. Therefore, the stain-controlled LCF tests on the smooth specimens were performed to obtain the LCF behaviour of TA19. Test temperature was 180 °C, being equal to the service temperature of the bolt hole in the compressor disc. Overviews of the LCF tests on smooth specimen and CHP specimen are given in Tables 2 and 3, respectively. The linear-elastic FE analysis was performed only to obtain the stress concentration factor, K_t. From Table 3, nearly the same values of K_t for all CHP specimens with different scales are observed, which is due to their similar notch geometries. For the purpose of comparison, all CHP specimens with different scales were tested at a nominal net section stress of 536.54 MPa, being equal to the stress value of the bolt hole in the compressor disc at service.

Table 2
Overview of the LCF tests on smooth specimen at $R_\varepsilon = 0.1$.

Maximum strain (%)	Minimum strain (%)	K_t	Number of specimens
1.6	0.16	1	2
1.4	0.14	1	3
1.2	0.12	1	4
1	0.1	1	3
0.8	0.08	1	1

Table 3
Overview of the LCF tests on CHP specimen at $R_\sigma = 0.1$.

Test section scale (%)	Nominal net section stress (MPa)	K_t	Number of specimens
100	634.94	2.321	4
100	588.70	2.321	4
100	536.54	2.321	5
100	496.72	2.321	4
100	450.73	2.321	4
80	536.54	2.336	4
60	536.54	2.353	4
40	536.54	2.357	5

3. Results

3.1. Fractography

Fractographic analysis was performed using scanning electronic microscope (SEM) on the gauge length of the specimens after frac-

ture to identify the characteristics of the fracture surfaces. For the sake of brevity, the fractography results for the smooth specimen and one representative CHP specimen were presented, as shown in Fig. 3. Three zones were observed for both specimens. Zone I includes the crack initiation region from surface (denoted by the white arrows) and crack propagation from the initial crack. Zone II shows further crack growth with the distinct characteristic of the fatigue failure, i.e., striations, which are the beach or clam shell markings on the cyclically grown portion of the fracture. Zone III is the final fast fracture area. Fatigue striations can be identified in both smooth specimen (see Fig. 4) and CHP specimen (see Fig. 5), indicating a transgranular fracture dominated fatigue failure.

3.2. LCF lifetime for smooth specimen

Fig. 6 plots the experimental data for TA19 smooth specimens under LCF loading at 180 °C within a broad strain range from 0.72% to 1.44%. It is shown that lifetime data under LCF loading lightly scatters due to the uncertainty related to the random distribution of defects in the test material.

The Basquin-Coffin-Manson equation widely used to describe the relationship between total strain range and fatigue life, is described by:

$$\frac{\Delta\varepsilon_t}{2} = \frac{\sigma'_f}{E}(2N_f)^b + \varepsilon'_f(2N_f)^c \tag{1}$$

where $\Delta\varepsilon_t$ is the total normal strain range, σ'_f is the fatigue strength coefficient, b is the fatigue strength exponent, ε'_f is the fatigue ductility coefficient, c is the fatigue ductility exponent.

When the mean stress is taken into account, the Smith-Watson-Topper (SWT) method in the plane of maximum normal strain range [25,26] is expressed as:

$$\frac{\Delta\varepsilon_t}{2}\sigma_{max} = \frac{(\sigma'_f)^2}{E}(2N_f)^{2b} + \sigma'_f\varepsilon'_f(2N_f)^{b+c} \tag{2}$$

in which σ_{max} is the maximum tensile stress in the critical plane.

The SWT parameter of TA19 at 180 °C was obtained based on the experimental data (see parameter values in Eq. (3)), in which σ_{max} was determined at the cycle number $N = N_f/2$.

$$\frac{\Delta\varepsilon_t}{2}\sigma_{max} = 97.628(2N_f)^{-0.578} + 10.272(2N_f)^{-0.105} \tag{3}$$

Meanwhile, the comparison of experimental data and predicted lifetime is shown in Fig. 7. The life scatter factor ΔN, defined in Eq. (4), was used to evaluate the accuracy of the life predictions. The SWT method gives a satisfactory prediction with the life scatter $\Delta N = 2.19$.

$$\Delta N = \max\left\{\frac{N_p}{N_e}(N_p > N_e), \frac{N_e}{N_p}(N_p \leqslant N_e)\right\} \tag{4}$$

3.3. LCF lifetime prediction for CHP specimen based on TCD

Experimental data for 100%-scale CHP specimen under the LCF loading is shown in Fig. 8. Similarly, scattering in lifetime data under different nominal net section stress levels was observed. The fitted curved is determined using the least square method. Considering the stress concentration in CHP specimen, traditional fatigue life prediction method based on the maximum stress/strain values would result in a significant deviation from the experimental data. Consequently, TCD concept initially proposed by Neuber [27] and Peterson [28] was employed to calculate an effective stress/strain at a given distance from the apex of the stress raiser instead of the maximum stress/strain. Applying this idea, a simplified way was then reformulated and concluded as the line method (LM) and the point method (PM) in the TCD by Taylor [9]. Taking as a starting point that the critical distance value varies with the number of cycles to failure, Susmel and Taylor [29,30] extended the use of TCD to the LCF regime.

The PM in terms of SWT parameter can be described as follows (see Fig. 9):

$$\left(\frac{\Delta\varepsilon_t}{2}\sigma_{max}\right)\Big|_{r=L} = \frac{(\sigma'_f)^2}{E}(2N_f)^{2b} + \sigma'_f\varepsilon'_f(2N_f)^{b+c} \tag{5}$$

where r is the distance to the notch tip, and L is the critical distance.

It is reported that TCD method combining with SWT parameter could successfully predict the fatigue lifetime of the notched specimen [31–33], due the SWT parameter was used to establish the relationship between fatigue life and damage parameter, while the TCD was introduced to consider the effect of the inhomogeneous stress/strain fields. In this regard, TCD concept was employed to predict the CHP specimen's LCF lifetime based on FE analysis in this study.

Commercial FE package ANSYS 14.0 was used to obtain the elastic-plastic stress/strain fields of the CHP specimen, where the

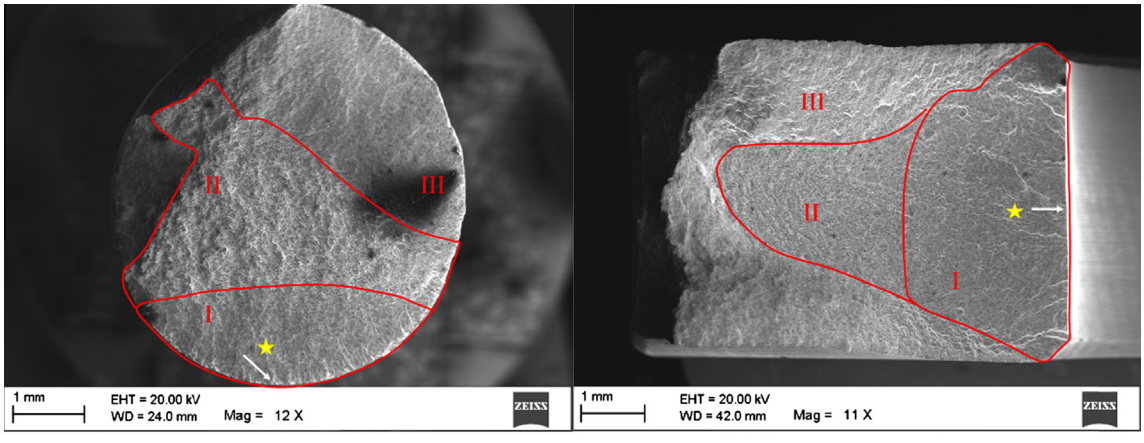

(a) (b)

Fig. 3. Micrograph of the fracture surfaces showing three zones: (a) smooth specimen under the maximum strain of 1.6%, (b) CHP specimen under the nominal net section stress of 634.94 MPa.

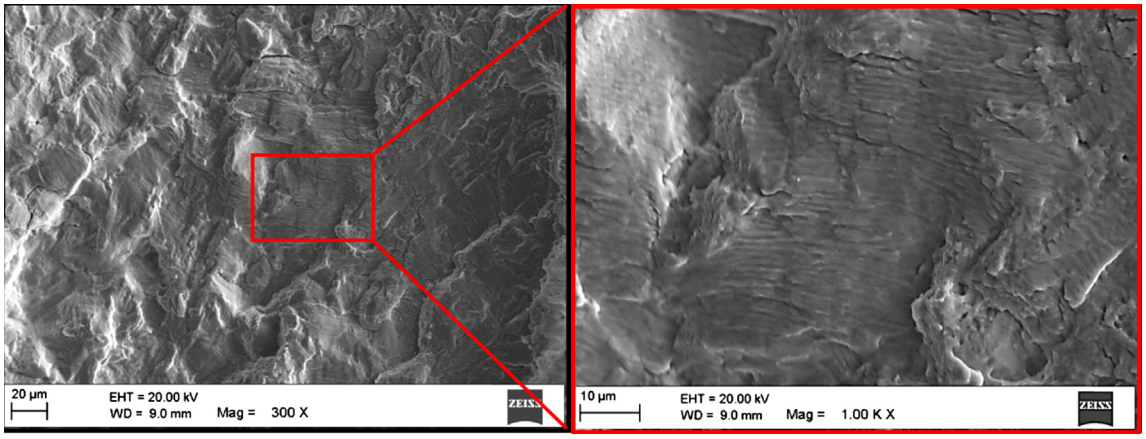

Fig. 4. SEM observation of fracture surface and its magnification of a smooth specimen at the maximum strain of 1.6%.

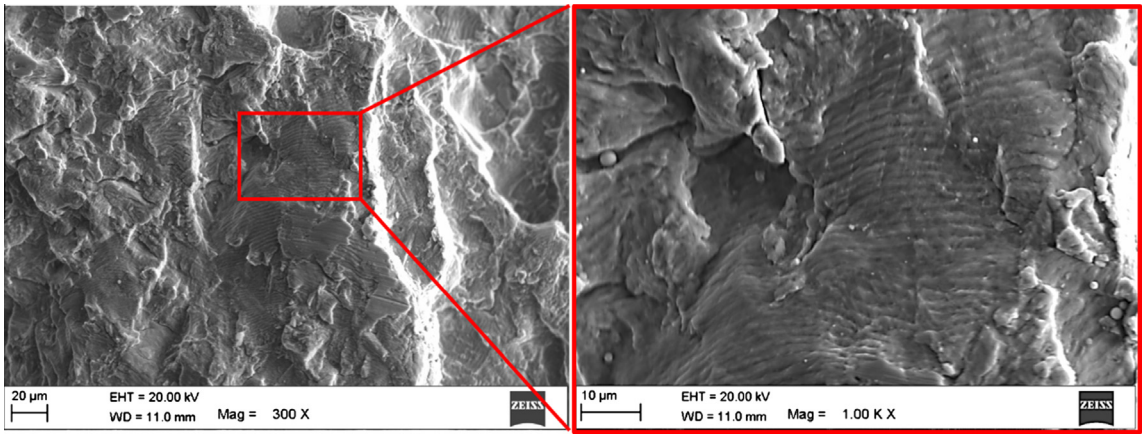

Fig. 5. SEM observation of fracture surface and its magnification of a representative CHP specimen at the nominal net section stress of 634.94 MPa.

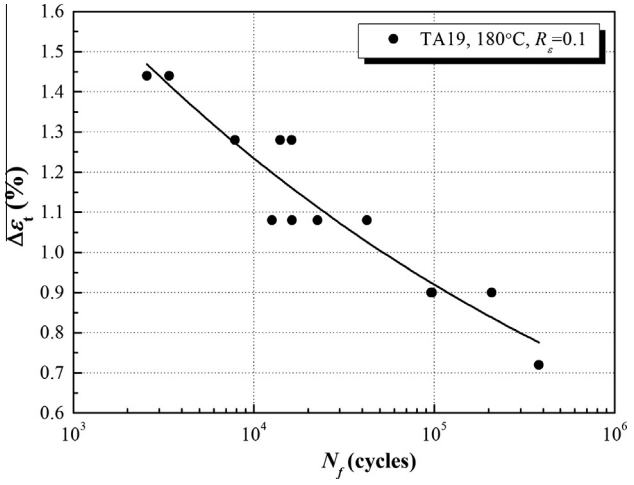

Fig. 6. Smooth specimen LCF test data of TA19 at 180 °C.

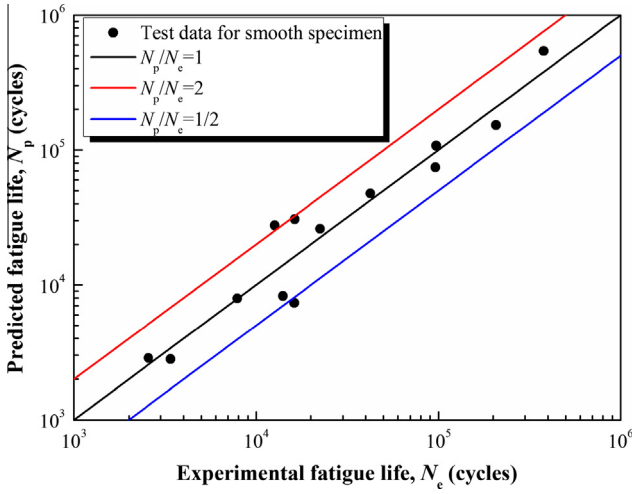

Fig. 7. Comparison between experimental data and predicted lifetime using SWT method.

multi-linear isotropic hardening rule was applied. Five cycles of loading were simulated to ensure the material in the area of stress concentration to reach a stabilized configuration. After loading, the strain range and maximum tensile stress in the critical plane were taken from the intersection line (i.e., the red line in Fig. 10) of the two symmetry planes of the specimen model.

Using SWT method, the calculated critical distance through a recursive procedure (See the detailed procedure in Ref. [29]) is shown in Fig. 11. The fitting curve was obtained using the least square method. Since the critical distance is determined by both the experimental data and the stress/strain fields around the notch, the critical distance shown in Fig. 11 scatters in two dimensions,

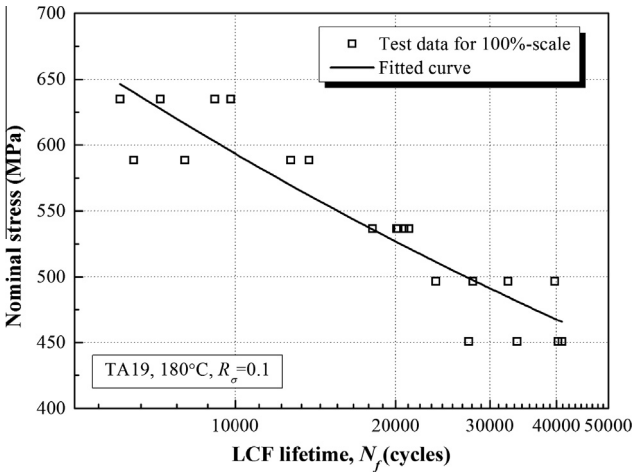

Fig. 8. The relationship between nominal net section stress and LCF lifetime for 100%-scale CHP specimen.

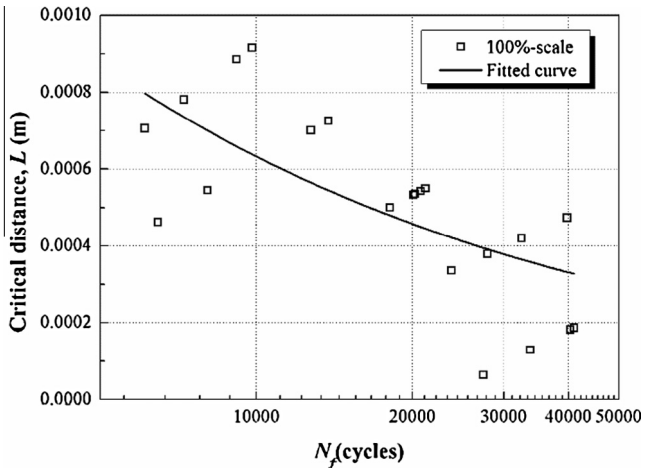

Fig. 11. Critical distances for 100%-scale CHP specimens.

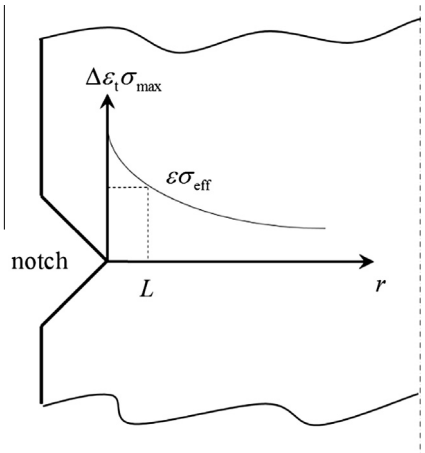

Fig. 9. Notched specimen subjected to nominal uniaxial fatigue loading: effective value of the strain amplitude and the maximum stress according to the PM.

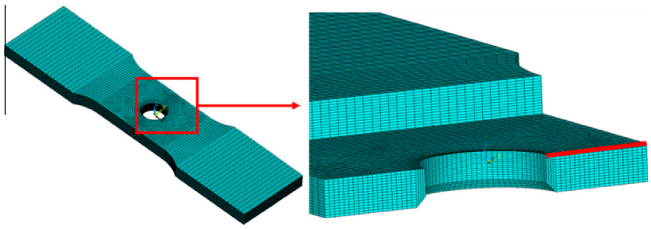

Fig. 10. The stress and strain data are extracted from the red line in the schematic picture. (For interpretation of the references to colour in this figure legend, the reader is referred to the web version of this article.)

i.e., fatigue life dimension and the nominal net section stress dimension, different from Fig. 8. The relationship between critical distance and fatigue life can be described by the following equation

$$L = AN_f^B \tag{6}$$

where A and B are material constants independent of the geometry features. For 100%-scale TA19 CHP specimens in this paper, $A = 0.0473$ and $B = -0.468$ while the unit of critical distance L is m.

Then the predicted LCF lifetime for 100%-scale CHP specimens is plotted in Fig. 12, with a life scatter factor $\Delta N = 2.16$, indicating a good correlation between the predicted and experimental data using the TCD model for 100%-scale CHP specimens.

3.4. Analysis on statistical size effect based on TCD

The fatigue lifetimes for CHP specimens with different scales under the same nominal net section stress loading exhibits a highly scale-dependent fatigue lifetime for TA19 notched specimens, as shown in Fig. 13. Consequently, the statistical size effect of the notched specimens on the LCF lifetime should be considered.

Using the established PM model based on the 100%-scale specimens in Eq. (6), the applicability of the TCD method to describe the statistical size effect was tested. Accordingly, the lifetimes for all of the four scales CHP specimens under the nominal net section stress of 536.54 MPa were predicted. For the sake of brevity, the predicted lifetime for different scales CHP specimens under the nominal net section stress of 536.54 MPa is shown in Fig. 14. The gaps for different scale CHP specimens are shown in Fig. 14. It was observed that the gap between predicted and experimental lifetimes increases as the scale of the specimen decreases. Moreover, the predicted LCF lifetime becomes more and more optimistic as the scale of the specimen decreases, which could lead to dangerous consequences in the engineering application of TCD.

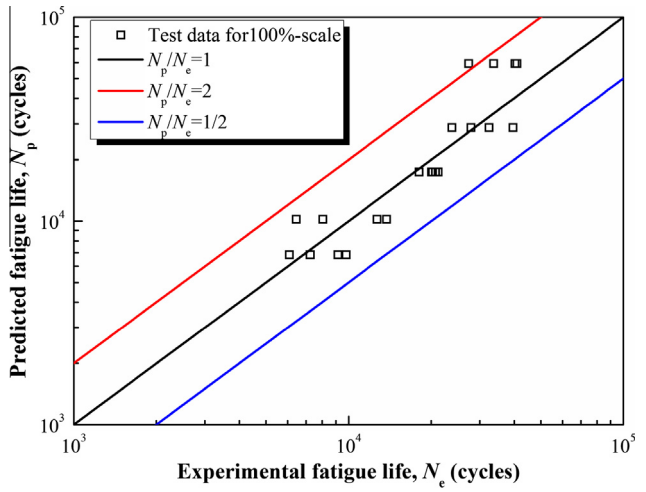

Fig. 12. Comparison between experimental data and the predicted results for the PM in the TCD.

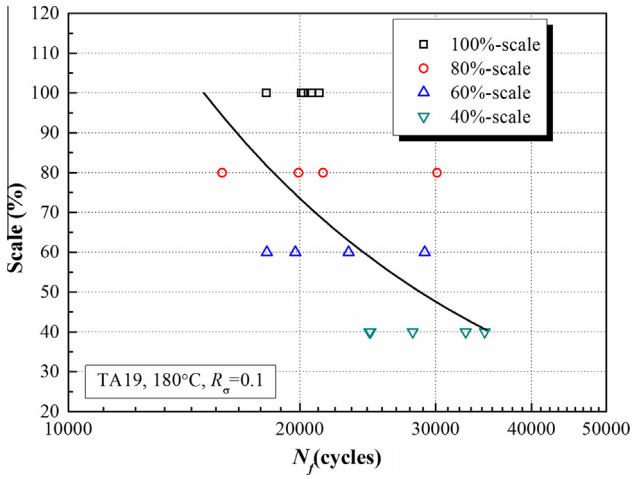

Fig. 13. The relationship between scale size of the test section and LCF lifetime for CHP specimens under the same nominal net section stress.

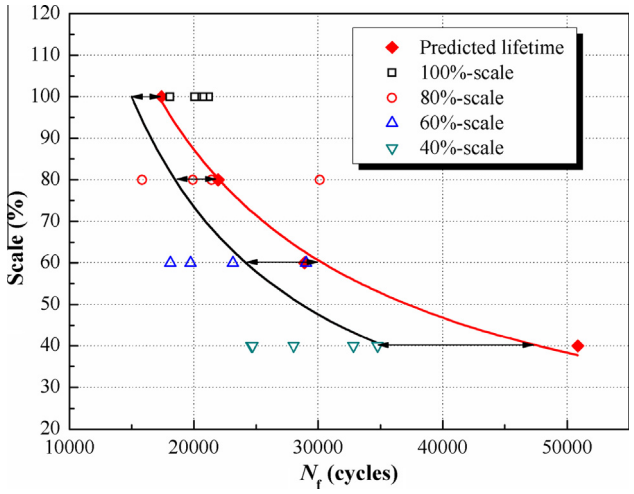

Fig. 14. Comparison of experimental and predicted lifetimes for different scales of CHP specimens. (The black line is the fitted curve for experimental lifetimes and the red line is the fitted curve for predicted lifetimes using the TCD method.). (For interpretation of the references to colour in this figure legend, the reader is referred to the web version of this article.)

An error index is introduced to assess the deviation between predicted and experimental lifetimes, that is

$$E_i = \log(N_{p,i}/N_{e,i}) \tag{7}$$

$$\overline{E} = \frac{1}{n}\sum_{i=1}^{n}|E_i| \tag{8}$$

where $\overline{E}$ is the average absolute error, E_i is the absolute error for the ith data, $N_{p,i}$ and $N_{e,i}$ are the predicted and experimental LCF lifetimes for the ith data respectively, n is the total data number.

The average absolute errors $\overline{E}$ of different scales of CHP specimens are listed in Table 4. A significant deviation ranges from 6.1% to 24.86% and the average absolute error for all of the test data is 13.02%, which means only employing TCD method is not enough to evaluate the statistical size effect. Therefore, it is necessary to introduce some more effective parameters with an improved accuracy in addition to TCD idea.

Table 4
The average absolute errors of PM.

Scale of CHP specimen (%)	Nominal net section stress (MPa)	Predicted lifetime (cycle)	Average absolute error (%)
100	536.54	17406	6.10
80		21952	8.28
60		28908	11.68
40		50853	24.86

3.5. Combined critical distance and highly-stressed-volume model

Volumetric approaches are effective in describing the statistical size effect [34]. As one of the mostly investigated methods in the evaluation of fatigue strength considering the statistical size effect and the geometrical size effect [34–36], the theory of highly-stressed-volume came into our sight. Kuguel [37] first introduced the idea of using the most highly-stressed-volume of a component for predicting its notched fatigue stress. More recently, Sonsino et al. [38] used V_{90}, which designates the volume with the stress amplitude $\sigma_a \geqslant 0.9\sigma_{a,max}$, to analyse the effect of size and notch in a variety of materials and components.

The 'V90 criterion' used to predict the fatigue strength is expressed as:

$$\frac{\sigma_A}{\sigma_{A0}} = \left(\frac{V_0}{V_{90}}\right)^v \tag{9}$$

where σ_A is the fatigue strength, σ_{A0} is the reference fatigue strength of a reference specimen with the reference volume V_0 and v is a material coefficient.

As a consequence, a novel model combining critical distance and highly-stressed-volume model, designated as LNV model, was proposed as the following

$$L = AN_f^B\left(\frac{V_{90}}{V_0}\right)^C \tag{10}$$

where C is a material constant. The highly-stressed-volume of 100%-scale CHP specimen is taken as the reference volume V_0. Thus, Eq. (10) can be simplified back to Eq. (6) when evaluating the fatigue life for the 100%-scale CHP specimen. The characteristic stress distribution caused by geometrical size effect is described by the calculation frame of TCD. The characteristic volume related to statistical size effect is described by the V_{90} obtained from linear-elastic FE analysis.

The recursive procedure to calculate N_p can be modified by highly-stressed-volume, as shown in Fig. 15. Different from the procedure in Ref. [29], V_{90} of the specimen is obtained as a necessary input at the beginning. A first attempt value of fatigue life, $N_{f,1}$, is assumed as another input of Eq. (10) to calculate the critical distance. Based on the elastic-plastic stress/strain fields around the notch, the SWT parameter at the critical distance is determined. Then a calculated fatigue life $N_{f,2}$ is calculated using Eq. (3). If the calculated $N_{f,2}$ is different from $N_{f,1}$, the procedure has to be performed by imposing $N_{f,1} = N_{f,2}$ until the result reaches a convergence.

$C = 0.213$ was obtained based on the test data for TA19 specimens under the nominal net section stress of 536.54 MPa. The predictive results using LNV model were compared with the original TCD, as plotted in Fig. 16. The average absolute errors of LNV model are listed in Table 5. It is shown from Fig. 16 and Table 5 that the predicted results are modified according to statistical size effect in four scales. The average absolute error of 40%-scale specimen is reduced from 24.86% to 6.06%. The average absolute error of all test data is also reduced from 13.02% to 10.31%.

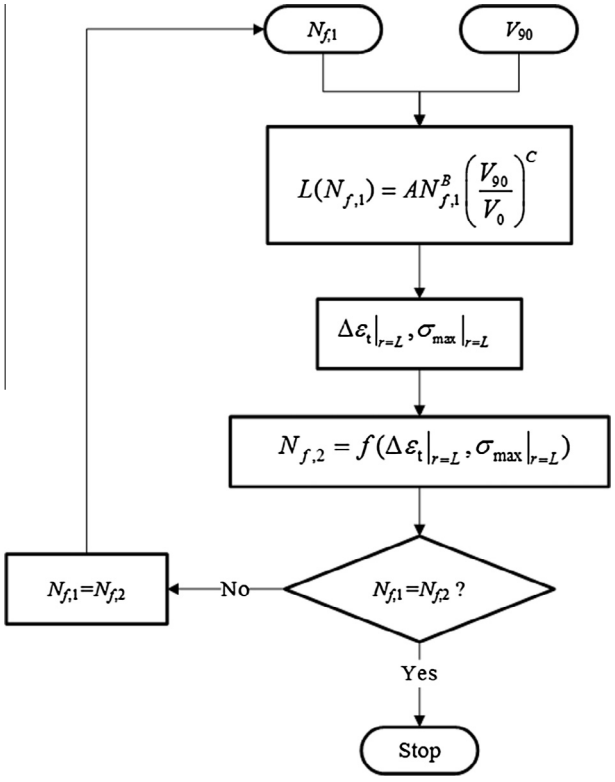

Fig. 15. Recursive procedure to calculate N_p modified by highly-stressed-volume.

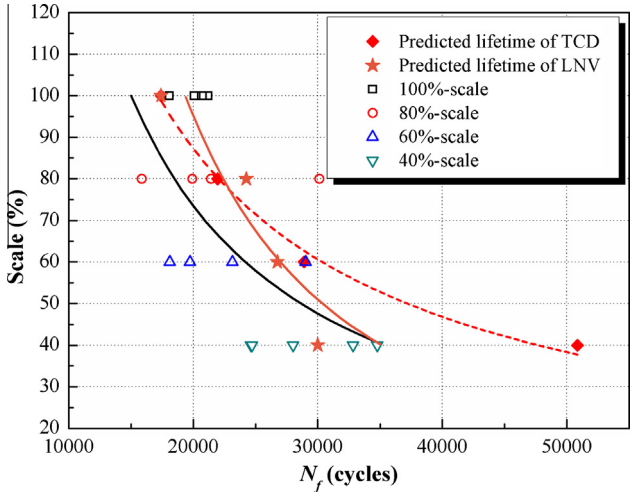

Fig. 16. Comparison of the prediction results between the TCD method and the LNV model under the nominal net section stress of 536.54 MPa. (The orange line is the fitted curve for predicted lifetimes using the LNV model.). (For interpretation of the references to colour in this figure legend, the reader is referred to the web version of this article.)

Table 5
The average absolute errors based on LNV model.

Scale of CHP specimen (%)	Nominal net section stress (MPa)	Predicted lifetime (cycle)	Average absolute error (%)
100	536.54	17405	6.10
80	536.54	21396	10.45
60	536.54	25556	9.98
40	536.54	38533	6.06

4. Discussions

It is observed from the test results of CHP specimens that the statistical size effect in LCF regime with stress concentration is evident in notch fatigue. Under the same nominal net section stress of 536.54 MPa, the average fatigue life of 40%-scale CHP specimens is 44.45% longer than that of 100%-scale CHP specimens. Though the comparisons were made under only one load level, the predictive results indicate the difference among the fatigue lives of specimens in different scales might possibly expand in the MCF and HCF regimes. Therefore, in the analysis of notch fatigue and the application of relevant analysis models, it is of critical importance to take the statistical size effect into account.

As a method with good adaptability, the TCD combined with SWT method in the critical plane gives a satisfactory life prediction for the 100%-scale specimen. The TCD can also distinguish the variations of fatigue life prediction for CHP specimens of different scales (see Fig. 14). However, without any consideration of statistical size effect, the prediction error is relatively large (Table 4). Moreover, the prediction error may keep increasing without control when the TCD model established from one scale of specimens is applied to other scale of specimens and other load levels.

Predicted results show that the average absolute error decreases as the scale of CHP specimens reduces. In the extreme case of smooth specimens with different sizes, the critical distances of smooth specimens are zero due to the homogeneous stress filed of the section area for TCD method, indicating the predicted lives of smooth specimens in different sizes are the same under the same load level. This conclusion contradicts the experimental observation of evident statistical size effect for smooth specimens reported in Ref. [39], which means the TCD could not reflect the statistical size effect of smooth specimens.

On the other hand, the introducing of the highly-stressed-volume in the LNV model is an essential supplement to the original TCD method. The predicted lifetimes under five load levels of the CHP specimens in four scales can be calculated using two models, as shown in Fig. 17. It is indicated from two overlapping curves of 100%-scale CHP specimen that the LNV model inherits the merits of the TCD. Meanwhile, the LNV model manages to give a modified prediction results for specimens in different scales under other loading levels considering the statistical size effect. Compared to the TCD, the minimization of the predictive error is improved using

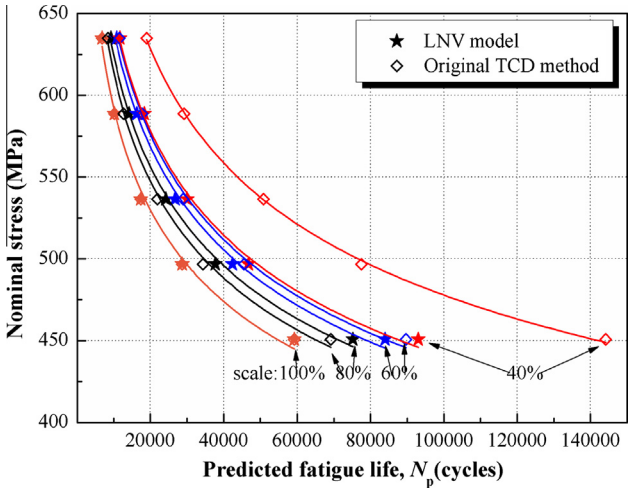

Fig. 17. Comparison of the prediction results between the TCD method and the LNV model under five load levels.

LNV model (see Fig. 16 and Table 5). Moreover, the proposed LNV model in the present study is feasible to describe the statistical size effect of smooth specimens.

Many modeling efforts have been made to analyse the geometrical size effect based on experimental results for different types of notch specimens. From the perspective of LNV model, the variations of notch type not only change the inhomogeneous stress distribution, but also change the highly-stressed-volume. That is, the geometrical size effect is always coupled with the statistical size effect in the fatigue assessment of specimens with different notch types. Therefore, it is necessary to choose a method, which can consider both geometrical and statistical size effect, to analyse the structures with different stress concentration factors.

5. Conclusions

In this study, an effective methodology to evaluate the statistical size effect of the stress concentrators on the LCF lifetime are developed by integrating critical distance and highly-stressed-volume model. The main results are summarized as follows:

(1) The TCD combined with SWT parameters in the critical plane reveals a good agreement with the test data for 100%-scale CHP specimens, with a life scatter factor, $\Delta N = 2.16$.
(2) Experimental lifetime for CHP specimens at different scales demonstrates the statistical size effect on the resultant fatigue life is evident. Under the same load of nominal net section stress, the average fatigue life of 40%-scale CHP specimens is 44.45% longer than the average fatigue life of 100%-scale CHP specimens.
(3) To address the statistical size effect, the theory of highly-stressed-volume is introduced to reformulate the original TCD. The statistical size effect is taken into account in the new LNV model. Compared to the life prediction results of the original TCD, the average absolute error of all test data is reduced from 13.02% to 10.31% using LNV model.
(4) The change of notch geometry is accompanied with the change of stress distribution and highly-stressed-volume. The geometrical size effect and statistical size effect should both be considered in the analysis of specimens with different notch types. More work has to be done to check the performance of LNV model when applying to other material, notch types and experimental conditions.

Acknowledgements

D. Hu and R. Wang acknowledge financial support from the National Natural Science Foundation of China (Grant Nos. 51675024, 51305012 and 51375031), Aviation Science Fund of China (Grant No. 2014ZB51) and Defense Industrial Technology Development Program (Grant No. B2120132006).

Appendix A. Supplementary material

Supplementary data associated with this article can be found, in the online version, at http://dx.doi.org/10.1016/j.ijfatigue.2016.10.003.

References

[1] FAA/SAE committee. Uncontained turbine engine rotor events; 1997.
[2] NTSB. Aircraft accident report (NTSB/AAR-90106). Natl Transp Saf Board; 1996. p. 1–126.
[3] Kloos KH. Einfluss des Oberflächenzustandes und der Probengröße auf die Schwingfestigkeitseigenschaften, VDI-Bericht 268, VDI-Verlag; 1976. p. 63–76.
[4] Leverant GR, McClung RC, Wu YT, Millwater HR, Riha DS, Enright MP, et al. Turbine rotor material design - final report. Washington, DC; 2000.
[5] Lorenzino P, Navarro A. Grain size effects on notch sensitivity. Int J Fatigue 2015;70:205–15.
[6] Liu X-Y, Su T-X, Zhang Y, Yuan M-N. A multiaxial high-cycle fatigue life evaluation model for notched structural components. Int J Fatigue 2015;80:443–8.
[7] Benedetti M, Fontanari V, Winiarski B, Withers PJ, Allahkarami M, Hanan JC. Fatigue behavior of shot peened notched specimens: effect of the residual stress field ahead of the notch root. Procedia Eng 2015;109:80–8.
[8] Baudoin P, Magnier V, El Bartali A, Witz J-F, Dufrenoy P, Demilly F, et al. Numerical investigation of fatigue strength of grain size gradient materials under heterogeneous stress states in a notched specimen. Int J Fatigue 2016;87:132–42.
[9] Taylor D. Geometrical effects in fatigue: a unifying theoretical model. Int J Fatigue 2000;21:413–20.
[10] Susmel L, Taylor D. The theory of critical distances to estimate lifetime of notched components subjected to variable amplitude uniaxial fatigue loading. Int J Fatigue 2011;33:900–11.
[11] Susmel L, Taylor D. A critical distance/plane method to estimate finite life of notched components under variable amplitude uniaxial/multiaxial fatigue loading. Int J Fatigue 2012;38:7–24.
[12] Susmel L, Taylor D. The theory of critical distances to estimate finite lifetime of notched components subjected to constant and variable amplitude torsional loading. Eng Fract Mech 2013;98:64–79.
[13] Yin T, Tyas A, Plekhov O, Terekhina A, Susmel L. A novel reformulation of the theory of critical distances to design notched metals against dynamic loading. Mater Des 2015;69:197–212.
[14] Lanning DB, Nicholas T, Haritos GK. On the use of critical distance theories for the prediction of the high cycle fatigue limit stress in notched Ti–6Al–4V. Int J Fatigue 2005;27:45–57.
[15] Lanning DB, Nicholas T, Palazotto A. The effect of notch geometry on critical distance high cycle fatigue predictions. Int J Fatigue 2005;27:1623–7.
[16] Yamashita Y, Ueda Y, Kuroki H, Shinozaki M. Fatigue life prediction of small notched Ti–6Al–4V specimens using critical distance. Eng Fract Mech 2010;77:1439–53.
[17] Wang JK, Yang XG. HCF strength estimation of notched Ti–6Al–4V specimens considering the critical distance size effect. Int J Fatigue 2012;10:97–104.
[18] Makkonen M. Statistical size effect in the fatigue limit of steel. Int J Fatigue 2001;23:395–402.
[19] Makkonen M. Notch size effects in the fatigue limit of steel. Int J Fatigue 2003;25:17–26.
[20] ISO 19902. Fixed steel structures; 2007.
[21]] API RP 2A-WSD. Recommended practice for planning, designing and constructing fixed offshore platforms – working stress design. 21st ed.; December 2000.
[22] DNV-RP-C203. Fatigue design of offshore steel structures; 2012.
[23] Coffin LF. A study of the effects of cyclic thermal stresses on a ductile metal. Trans ASME 1954;76:931–50.
[24] Manson SS. Behavior of materials under conditions of thermal stress. NACA Report (NACA TN-2933); 1953.
[25] Socie D. Multiaxial fatigue damage models. J Eng Mater Technol 1987;109(4):293–8.
[26] Smith KN, Watson P, Topper TH. A stress-strain function for the fatigue of metals. J Mater 1970;5:767–76.
[27] Neuber H. Theory of notch stresses: principles for exact calculation of strength with reference to structural form and material. 2nd ed. Berlin: Springer Verlag; 1958.
[28] Peterson RE. Notch sensitivity. In: Sines G, Waisman JL, editors. Metal fatigue. New York: McGraw Hill; 1959. p. 293–306.
[29] Susmel L, Taylor D. A novel formulation of the theory of critical distances to estimate lifetime of notched components in the medium-cycle fatigue regime. Fatigue Fract Eng Mater Struct 2007;30(7):567–81.
[30] Susmel L, Taylor D. An elasto-plastic reformulation of the theory of critical distances to estimate lifetime of notched components failing in the low/medium-cycle fatigue regime. J Eng Technol 2010;132(2):210021–8.
[31] Yang XG, Wang JK, Liu JL. High temperature LCF life prediction of notched DS Ni-based superalloy using critical distance concept. Int J Fatigue 2011;33:1470–6.
[32] Leidermark D, Moverare J, Segersall M, Simonsson K, Sjöström S, Johansson S. Evaluation of fatigue crack initiation in a notched singlecrystal superalloy component. Procedia Eng 2011;10:619–24.
[33] Leidermark D, Moverare J, Simonsson K, Sjöström S. A combined critical plane and critical distance approach for predicting fatigue crack initiation in notched single-crystal superalloy components. Int J Fatigue 2011;33:1351–9.
[34] Härkegård G, Halleraker G. Assessment of methods for prediction of notch and size effects at the fatigue limit based on test data by Böhm and Magin. Int J Fatigue 2010;32:1701–9.
[35] Lin CK, Lee WJ. Effects of highly stressed volume on fatigue strength of austempered ductile irons. Int J Fatigue 1998;20:301–7.

[36] Kaffenberger M, Vormwald M. Considering size effects in the notch stress concept for fatigue assessment of welded joints. Int J Fatigue 2012;64:71–8.
[37] Kuguel R. A relation between theoretical stress concentration factor and fatigue notch factor deduced from the concept of highly stressed volume. Proc ASTM 1961;61:732–48.
[38] Sonsino CM, Kaufmann H, Grubišić V. Transferability of material data for the example of a randomly loaded forged truck stub axle. SAE Technical Paper Series 1997. doi: http://dx.doi.org/10.4271/970708.
[39] Shirani M, Härkegård G. Fatigue life distribution and size effect in ductile cast iron for wind turbine components. Eng Fail Anal 2011;18:12–24.